International Journal of Engineering Trends and Technology
ISSN: 2231–5381 / https://doi.org/10.14445/22315381/IJETT-V73I2P104

Volume 73 Issue 2, 39-45, February 2025

Original Article

AFM and Raman Studies of Chemical Bath Deposited Nickel Sulphide Films

Ho Soonmin[1], K. Mohanraj[2]

[1]*Faculty of Health and Life Sciences, INTI International University, Putra Nilai, Malaysia.*
[2]*Department of Physics, Central University of Tamil Nadu, Thiruvarur, India.*

[1]*Corresponding Author : soonmin.ho@newinti.edu.my*

Received: 21 August 2024 Revised: 14 November 2024 Accepted: 20 January 2025 Published: 21 February 2025

Abstract - *Nickel sulphide thin films were deposited onto microscope glass substrate through chemical bath deposition method in acidic conditions. In this work, nickel sulphate and sodium thiosulfate were employed as reaction starting materials to produce binary compounds. Different solution concentrations (0.075 M, 0.1 M, and 0.15 M) and deposition times (12 hours and 33 hours) were used to investigate the properties of films for the first time. According to the Atomic Force Microscopy analysis, the best morphology could be observed when the films were prepared using 0.1M of solution, 12 hours and 33 hours, respectively. These films indicated uniform morphology and homogeneous surface if compared to other samples. Based on Raman spectroscopy results, the highest intensity could be recorded for these samples also.*

Keywords - *Photovoltaic, Renewable energy, Energy efficiency, Thin films, Solar cell applications, Semiconductor materials, Energy consumption.*

1. Introduction

In the past decade, many types of semiconductor compounds have been reported for laser devices, photovoltaic industry [1], sensor devices [2], optoelectronic devices [3], and solar selective coatings. These films attract researchers' attention due to unique properties [4], production costs [5] and final applications. Several chemical deposition techniques have been demonstrated by researchers to prepare thin films. Generally, these deposition techniques could be categorized into gas phase and liquid phase deposition. Examples of gas phases such as atomic layer epitaxy [6] and chemical vapor deposition [7]. While examples of liquid phase including sol-gel [8], dip coating, spin coating [9], chemical bath deposition, anodic oxidation and spray pyrolysis [10]. It was noticed that the properties of prepared films could be controlled using chemical bath deposition method. Researchers have reported that composition, film thickness, geometry, and morphology could be adjusted easily by using this low-cost method [11]. Therefore, this method can play an important role in the field of nanomaterials, especially to form desired products in the nanometer scale [12]. Atomic Force Microscopy (AFM) is recommended as a valuable tool for analyzing the topographical characteristics of samples in nanotechnology [13]. Its advantages include not requiring conductive samples, the ability to magnify in all three axes, and the capability to function in air or liquid environments [14]. AFM can produce high-resolution 3D images, even at the atomic level. Its operation is based on sensing the forces between the sharp tip and the sample surface, which can be either attractive or repulsive, and is heavily influenced by the operating modes. In contact mode, the AFM probe tip maintains high-resolution contact with the sample surface [15]. The interaction between the AFM tip and the surface is predominantly repulsive. Many benefits have been highlighted, including the ability to scan rough samples at a high speed. When operating in non-contact mode, the AFM tip oscillates without making physical contact with the sample, thereby minimizing the interaction between the tip and the sample [16]. Tapping mode involves the AFM tip oscillating and making intermittent contact with the sample surface. This mode offers advantages such as higher lateral resolution, minimal lateral forces, reduced overall forces, and less sample damage [17]. Ultimately, the quality of the imaging heavily relies on choosing the appropriate operation mode. Notably, tapping mode is applicable in biomedical contexts. Avoid contact mode as it can distort biomedical samples during scanning. Conventional AFM imaging is time-consuming and can take several attempts to produce a single image [18]. Biomedical samples require higher frame rates for imaging due to the rapid biological processes that can occur within milliseconds [19]. High-bandwidth scanners have been developed to improve imaging speed. Optimizing imaging parameters such as line speed, frame rate, spatial resolution, range, and pixel resolution will lead to better performance. A non-destructive method of chemical investigation, Raman Spectroscopy yields precise data on molecular interactions, phase and polymorphy, crystallinity, and chemical structure

[20]. It is predicated on how light interacts with a material's chemical connections. A molecule scatters incident light from a high intensity laser light source using the Raman technique of light scattering [21]. Rayleigh scattering is the term for most of the scattered light that is at the same wavelength as the laser source and does not offer any meaningful information [22]. Raman scatter is the minuscule quantity of light that is scattered at various wavelengths depending on the analyte's chemical structure [23]. Nickel sulfide is utilized in solar cells due to its conductivity, electrochemical characteristics and affordability. The produced p-type semiconductor films are suitable for solar cell applications because of excellent absorption characteristics, including a higher absorption coefficient, appropriate band gap value, and clear quantum size effects along with refractive index values.

In this work, we report the impact of deposition time (12 hours and 33 hours) and solution concentration (0.0075 M, 0.1 M and 0.15 M) on properties of nickel sulphide thin films. These films have been grown onto microscope slides using chemical bath deposition method. During the formation of thin films, nickel sulphate and sodium thiosulphate were used to provide nickel ions and sulphide ions, respectively. The fabricated films were studied using Raman spectroscopy and atomic force spectroscopy technique to investigate the phase and topography properties, respectively, for the first time.

2. Methodology

In this work, nickel (II) sulphate, sodium thiosulphate, hydrochloric acid, and sodium hydroxide were used. The glass substrate (microscope glass) was rinsed, cleaned and used for deposition of nickel sulphide films. During the experiment, nickel sulphate and sodium thiosulphate were put in a beaker. Then, the cleaned substrate was vertically immersed in the beaker. Here, different deposition times (12 hours and 33 hours) and solution concentration (0.0075 M, 0.1 M and 0.15 M) were selected to investigate the properties of films. Chemical bath deposition of films was carried out at 23 °C when the pH was 4 without using complexing agent. Desire pH value could be adjusted using hydrochloric acid, and sodium hydroxide solution. Topography properties of the prepared films were studied using atomic force microscopy technique (contact mode, model's name= NX-10 and manufacturer=Park system). On the other hand, the phases of the obtained samples were investigated using Raman microscope model LabRam HR evolution (Horiba) and the laser excitation of 325 nm (Helium Cadmium).

3. Results and Discussion

The metallic element nickel has a glossy, silvery-white look. It is widely distributed throughout the crust and core of the planet, making it the sixth most frequent element there [24]. Iron and nickel are both frequently found elements in meteorites. Both soil and water naturally contain nickel. It is also a nutrient that plants require. A common mineral in soil, water, and air is nickel. It is a part of several enzymes in the human body that are engaged in chemical processes and may help with the absorption of iron. The most frequent side effect is an allergic response that manifests as a rash that itches (contact dermatitis). This may occur in areas of your body where you are not directly exposed to nickel [25], such as areas where your skin comes into touch with it.

The chemical element sulphur has the atomic number sixteen and the symbol S. It is nonmetallic, multivalent, and plentiful [26]. Sulphur atoms normally combine to create cyclic octatomic molecules, which have the chemical formula S_8. At room temperature, elemental sulphur is a crystalline solid that is brilliant yellow in colour. People are not very poisonous to sulphur. On the other hand, consuming too much sulphur might result in diarrhoea or a burning feeling. Sulphur dust inhalation can irritate the respiratory tract or induce coughing. Additionally, it may irritate the eyes and skin [27]. Utilising the chemical reaction-in which the result self-assembles and deposits on an appropriate substrate-chemical deposition makes use of this process. Thin nanostructured mix films of crystalline inorganic materials with a variety of morphologies, including nanorods, nanotubes, nanopins, and nanospheres, are often created via chemical deposition [28].

One method of manufacturing is chemical deposition, in which the material to be coated is exposed to various chemicals, causing certain reactions to occur that lead to the effective formation of the coating. Chemical bath deposition, electrodeposition, successive ionic layer adsorption and reaction [29], chemical reduction, sol–gel method, chemical vapour deposition, and dip coating are a few examples of the various forms that chemical deposition can take. Precursors of the species being deposited are used in the deposition process known as chemical bath deposition. In its most basic version, heating and stirring substrate holding fixtures and solution containers are needed [30].

The precursor solution is submerged in the substrate, and then the mixture is heated, agitated, and hydrolysed. Particle growth and nucleation take place at the substrate's surface [31]. Temperature and deposition time adjustments can be used to regulate the size, shape, morphology, and thickness of the films [32]. Films that are stable, homogenous, adherent, and have good repeatability are produced by this method [33]. Different solution concentrations were used to prepare thin films for a duration of 12 hours and was reported for the first time. Significant morphology will be seen after scanned at specific areas (10 μm X 10 μm), as indicated in Figure 1 (a)-(c) and Figure 2 (a)-(c), representing 2-dimensional and 3-dimensional images, respectively. It was discovered that increasing the concentration from 0.075 M to 0.1 M enhanced the film coverage. It was noted that it is significantly discontinuous with a mass of irregular grains with micro-scale holes could be formed when the concentration was 0.0075 M for 12 hours (Figure 1(a), 2(a)). RMS roughness will be reported as 0.0159 μm. In addition, more grains could be

observed when the films were prepared using higher concentration (concentration was 0.15 M), resulted in higher RMS roughness value (roughness=0.016 μm). Good coverage has been linked to improved solar cell performance, according to research [34]. Zhao and co-workers have highlighted that the presence of numerous holes resulted in serious charge recombination process. They concluded that full surface coverage [35] was enhanced by high-performance perovskite solar cells.

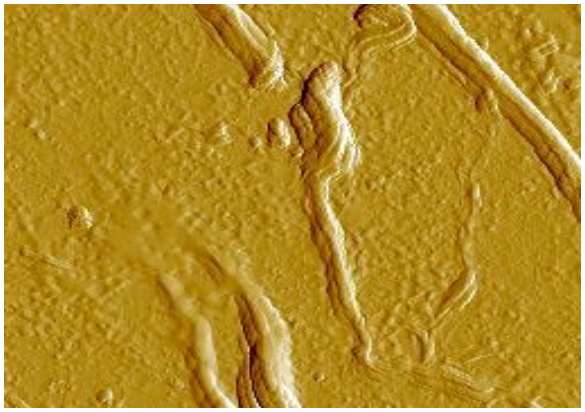

(a)

(b)

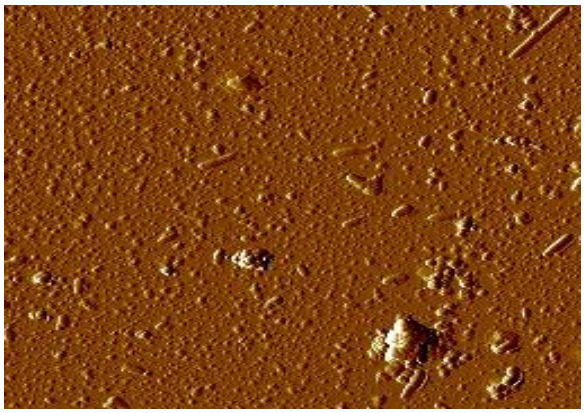

(c)

Fig. 1 The 2-dimensional of AFM images of the films deposited using different concentrations for 12 hours (a) 0.0075 M, (b) 0.1 M, and (c) 0.15 M

As shown in Figures 1(b), and 2(b), the prepared samples were obviously homogeneous, full surface coverage and continual with increasing the precursor solution concentration (0.1 M). Also, these films showed the smoothest morphology (surface roughness=0.001 μm) if compared to other samples. Because of their non-cracking structure, these films were suitable for use in solar cell applications [36].

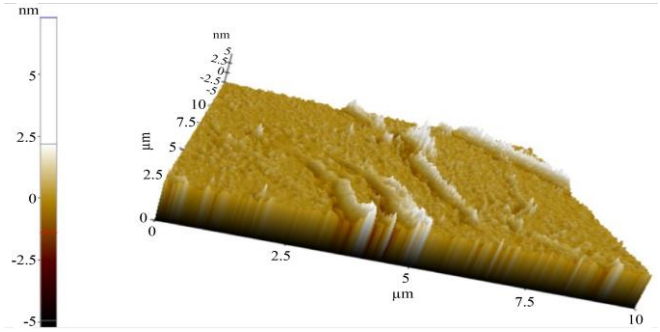

(a)

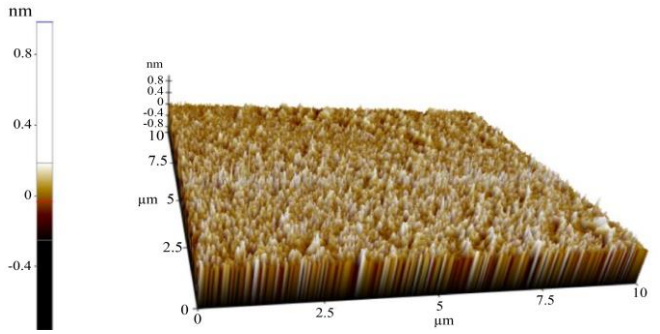

(b)

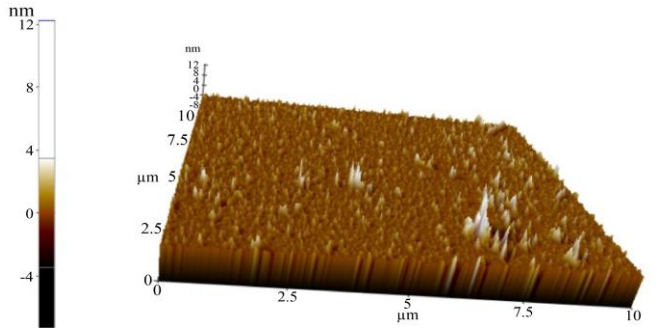

(c)

Fig. 2 The 3-dimensional of AFM images of the films deposited using different concentrations for 12 hours (a) 0.0075 M, (b) 0.1 M, and (c) 0.15 M

On the other hand, morphology of the films deposited using different concentrations for 33 hours was studied (Figure 3, and Figure 4). As shown in AFM images, prepared films relatively bigger grains could be found when the solution concentration was 0.15 M. Many researchers [37, 38] have explained that larger grains can improve charge transporting behaviours because of the enlarge contact area. When the concentration reached 0.0075 M for 33 hours, it was seen to be considerably discontinuous with a mass of irregular grains that may produce micro-scale holes (Figure 3(a), 4(a)). On the other hand, AFM results confirmed that uniform films with the

smallest RMS roughness value (0.0004 μm) could be found when the concentration was 0.1 M. Higher RMS roughness value (roughness=0.016 μm) was reported when the concentration was 0.0075 M because of mixing different particle sizes.

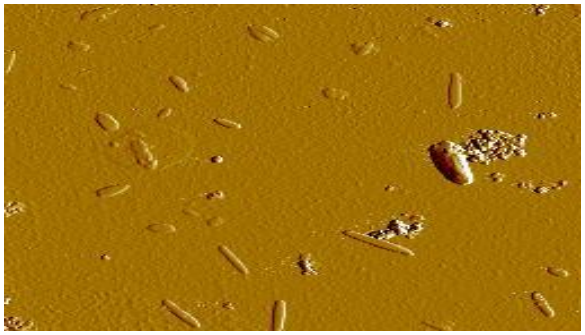

(a)

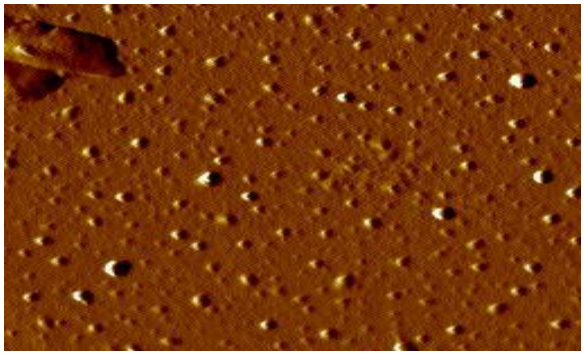

(b)

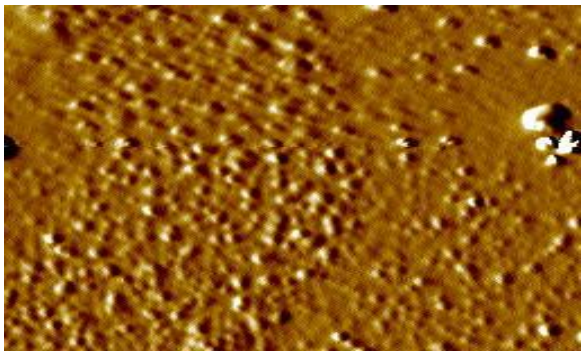

(c)

Fig. 3 The 2-dimensional of AFM images of the films deposited using different concentrations for 33 hours (a) 0.0075 M, (b) 0.1 M, and (c) 0.15 M

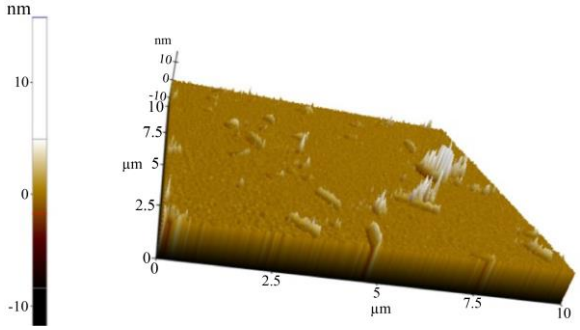

(a)

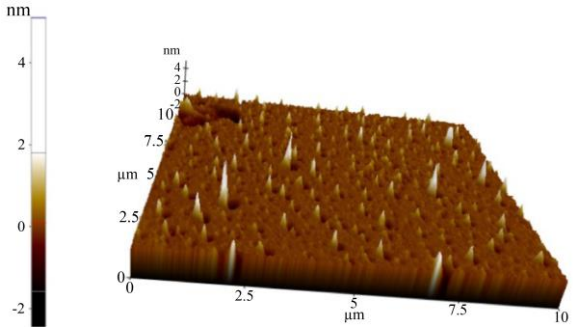

(b)

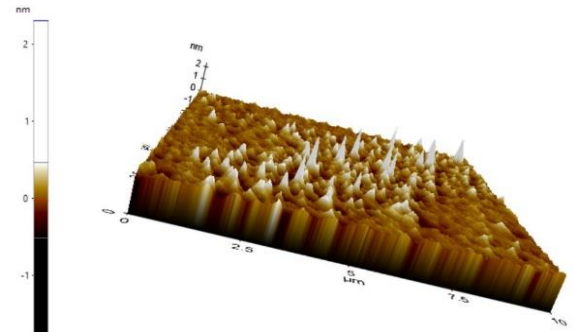

(c)

Fig. 4 The 3-dimensional of AFM images of the films deposited using different concentrations for 33 hours (a) 0.0075 M, (b) 0.1 M, and (c) 0.15 M

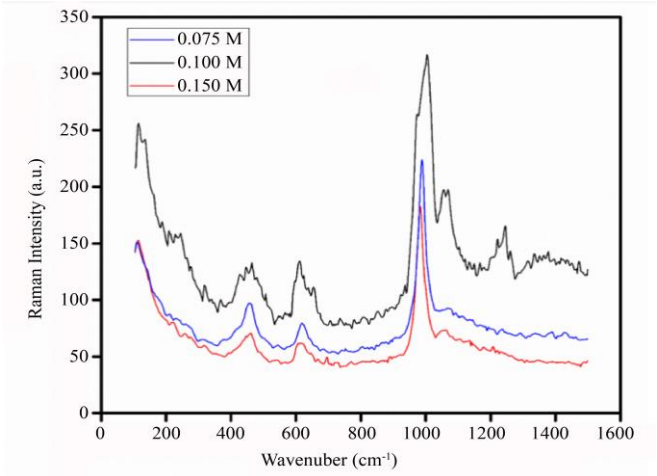

Fig. 5 Raman spectra of films prepared using various concentrations for 12 hours

It can be seen from the Raman spectra (Figure 5) that vibrational bands around 220 cm^{-1}, 285 cm^{-1}, 489 cm^{-1}, 596 cm^{-1}, 990 cm^{-1} and 1087 cm^{-1} are attributed to A1g, Eg, and Tg active modes of vibration of nickel sulfide [39-43]. The characteristic peak is shown at 489 cm^{-1} due to TO mode of vibration. Among the peaks at 489 cm^{-1} and 596 cm^{-1} are both broad and asymmetrical vibrations and are due to Raman active optical phonons. It is noticed that intensity variation and peak shift with varying concentrations of the samples confirm the active vibrations that take place in the synthesized samples.

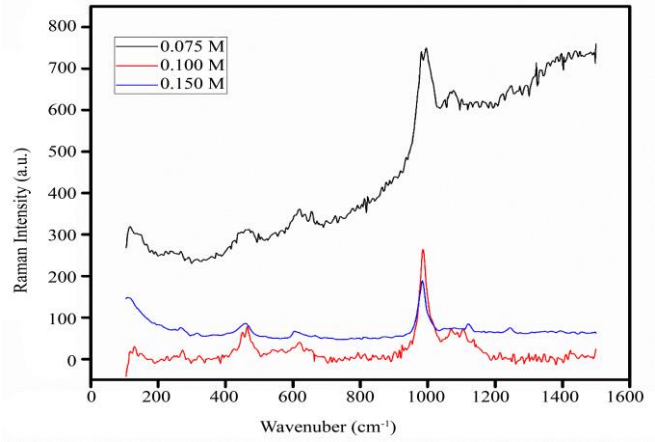

Fig. 6 Raman spectra of films prepared using various concentrations for 33 hours

Among the concentrations, 0.1M could be found to have a better result, and similarly, the intensity of vibrational bands (Figure 6) varies with the deposition time. Raman analysis confirms the formation of the nickel sulfide thin film on the substrate.

4. Conclusion

Nickel sulfide thin films could be used in solar cells, supercapacitors, lithium batteries and many applications. These films have been prepared using various types of deposition methods. In this work, binary nickel sulfide films were synthesized using chemical bath deposition technique (time= 12 hours and 33 hours, concentration of solution = 0.075M, 0.1 M, and 0.15 M). The properties of the obtained films were studied using atomic force microscopy and Raman spectroscopy for the first time. Overall results confirmed that better quality of films could be produced using higher concentration.

Funding Statement

This research work (Ho SM) was financially supported by a research grant (INTI IU Research Seeding Grant 2022: INTI-FHLS-12-02-2022).

Acknowledgments

This research work was financially supported by INTI International University (Ho SM).

References

[1] Yanhui Dong et al., "Efficiency Enhancement in CIGS Solar Cells with Ferroelectric $BiFeO_3$ Nanoparticles and $Mg_{0.07}Zn_{0.93}O/Mg_{0.12}Zn_{0.88}O$ Bilayer Window," *Chemical Engineering Journal*, vol. 495, 2024. [CrossRef] [Google Scholar] [Publisher Link]

[2] Ahmad Umar et al., "Fabrication and Characterization of CuO Nanoplates Based Sensor Device for Ethanol Gas Sensing Application," *Chemical Physics Letters*, vol. 763, 2021. [CrossRef] [Google Scholar] [Publisher Link]

[3] Ammar Qasem et al., "Characterization of Structural, Optical, Sensing, and Electrical Implications of Mn-ion Introducing in $Mn_xSe_{75-x}S_{25}$ thin Films for Optoelectronic and Gas Sensor Applications," *Optik*, vol. 300, 2024. [CrossRef] [Google Scholar] [Publisher Link]

[4] Alok Kumar et al., "Designing and Simulating of New Highly Efficient Ultra-Thin CIGS Solar Cell Device Structure: Plan to Minimize Cost per Watt Price," *Journal of Physics and Chemistry of Solids*, vol. 193, 2024. [CrossRef] [Google Scholar] [Publisher Link]

[5] S.M. Ho, and I. Hassan, "Lead Free Perovskite Materials for Solar Cell: An Update ofRecent Trends," *International Journal of Thin Film Science and Technology*, vol. 11, no. 3, pp. 283-292, 2022. [CrossRef] [Google Scholar] [Publisher Link]

[6] Gulcin Bolat et al., "Controllable Synthesis of Ag_2Se Binary Thin-Film via Electrochemical Atomic Layer Epitaxy (ECALE) and its Characterization," *Materials Chemistry and Physics*, vol. 318, 2024. [CrossRef] [Google Scholar] [Publisher Link]

[7] Wei-Long Xu et al., "Tin-based Perovskite Films Fabricated by Chemical Vapor Deposition for Photodetector Application," *Chemical Physics*, vol. 580, 2024. [CrossRef] [Google Scholar] [Publisher Link]

[8] Igor A. Pronin et al., "Sol-gel Derived ZnO Film as a Gas Sensor: Influence of UV Processing Versus a Thermal Annealing," *Sensors and Actuators A: Physical*, vol. 377, 2024. [CrossRef] [Google Scholar] [Publisher Link]

[9] Junaid Saleem et al., "Advancing Spin-Coating Technique for Semi-Crystalline Low-Density Polyethylene Thin Films," *Materials Today Proceedings*, 2024. [CrossRef] [Google Scholar] [Publisher Link]

[10] Md. Hasnat Rabbi et al., "Growth of High Quality Polycrystalline InGaO Thin Films by Spray Pyrolysis for Coplanar Thin-Film Transistors on Polyimide Substrate," *Journal of Alloys and Compounds*, vol. 1002, 2024. [CrossRef] [Google Scholar] [Publisher Link]

[11] T. Nimalan, and M.R. Begam, "Physical and Chemical Methods: A Review on the Analysis of Deposition Parameters of Thin Film Preparation Methods," *International Journal of Thin Films Science and Technology*, vol. 13, no. 1, pp. 59-66, 2024. [CrossRef] [Google Scholar] [Publisher Link]

[12] M.A. Vicencio Garrido et al., "Low-cost Chemical Bath Deposition Synthesis of Zinc Oxide/Zinc Sulfide Composite and Zinc Hydrozincite for Methylene Blue Degradation," *Inorganic Chemistry Communications*, vol. 164, pp. 1-9, 2024. [CrossRef] [Google Scholar] [Publisher Link]

[13] Erveton P. Pinto et al., "Comparing the Nanoscale Topography and Interface Properties of Chitosan Films Containing Free and Nano-Encapsulated Copaiba Essential Oil: An Atomic Force Microscopy (AFM) and Fractal Geometry Study," *Materials Today Communications*, vol. 35, 2023. [CrossRef] [Google Scholar] [Publisher Link]

[14] Hongwei Luo et al., "An AFM-IR Study on Surface Properties of Nano-TiO_2 Coated Polyethylene (PE) Thin Film as Influenced by Photocatalytic Aging Process," *Science of The Total Environment*, vol. 757, 2021. [CrossRef] [Google Scholar] [Publisher Link]
[15] Tram Nhu Hoang Tran et al., "C-AFM Study on Multi - Resistive Switching Modes Observed in Metal-Organic Frameworks Thin Films," *Organic Electronics*, vol. 93, 2021. [CrossRef] [Google Scholar] [Publisher Link]
[16] Yongda Yan et al., "Modelling and Experimental Study of Nanoscratching Process on PMMA Thin-Film using AFM Tip-based Nanomachining Approach," *Precision Engineering*, vol. 54, pp. 138-148, 2018. [CrossRef] [Google Scholar] [Publisher Link]
[17] Xinshuang Gao et al., "In Situ Differential Atomic Force Microscopy (AFM) Measurement for Ultra-Thin Thiol SAM Patterns by Area-Selective Deposition Technique" *Surfaces and Interfaces*, vol. 46, 2024. [CrossRef] [Google Scholar] [Publisher Link]
[18] Robinson Franco Alvarez, and Maria Cecilia Barbosa da Silveira Salvadori, "Using AFM to Measure the Elastic Modulus of Diamond-Like Carbon thin Films," *Diamond and Related Materials*, vol. 145, 2024. [CrossRef] [Google Scholar] [Publisher Link]
[19] Eleonora Bettini et al., "Influence of Metal Carbides on Dissolution Behavior of Biomedical CoCrMo Alloy: SEM, TEM and AFM Studies," *Electrochimica Acta*, vol. 56, no. 25, pp. 9413-9419, 2011. [CrossRef] [Google Scholar] [Publisher Link]
[20] S. Das et al., "Temperature Dependent Raman and Photoresponse Studies of Bi_2Te_3 Thin Films Annealed at Different Temperatures for Improved Optoelectronic Performance," *Materials Advances*, vol. 5, pp. 3379-3395, 2024. [CrossRef] [Google Scholar] [Publisher Link]
[21] Fiza Mumtaz et al., "Raman Spectroscopy Study and Dielectric Anomalies in $Bi_{1-x}Eu_x$ AFM FeO_3 Thin Films," *Thin Solid Films*, vol. 789, 2024. [CrossRef] [Google Scholar] [Publisher Link]
[22] Devesh Kumar Pathak et al., "Raman Area- and Thermal-Mapping Studies of Faceted Nano-Crystalline α-Fe_2O_3 Thin Films Deposited by Spray Pyrolysis," *Canadian Journal of Chemistry*, vol. 100, no. 7, pp. 507-511, 2021. [CrossRef] [Google Scholar] [Publisher Link]
[23] Chandra Bhal Singh et al., "Defect Study of Phosphorous Doped a-Si:H Thin Films using Cathodoluminescence, IR and Raman Spectroscopy," *Journal of Non-Crystalline Solids*, vol. 605, 2023. [CrossRef] [Google Scholar] [Publisher Link]
[24] Hua Chen et al., "Removal Process of Nickel(II) by using Dodecyl Sulfate Intercalated Calcium Aluminum Layered Double Hydroxide," *Applied Clay Science*, vol. 132-133, pp. 419-424, 2016. [CrossRef] [Google Scholar] [Publisher Link]
[25] Jinhua Ou et al., "Fabrication of Nickel-Iron Layered Double Hydroxides using Nickel Plating Wastewater via Electrocoagulation, and its Use for Efficient Dye Removal," *Journal of Molecular Liquids*, vol. 335, 2021. [CrossRef] [Google Scholar] [Publisher Link]
[26] Young Sun Mok, and Heon-Ju Lee, "Removal of Sulfur Dioxide and Nitrogen Oxides by using Ozone Injection and Absorption–Reduction Technique," *Fuel Processing Technology*, vol. 87, no. 7, pp. 591-597, 2006. [CrossRef] [Google Scholar] [Publisher Link]
[27] Cunhua Ma et al., "Oxidative Desulfurization of a Model Fuel using Ozone Oxidation Generated by Dielectric Barrier Discharge Plasma Combined with Co_3O_4/γ-Al_2O_3 Catalysis," *RSC Advances*, vol. 5, no. 117, pp. 96945-96052, 2015. [CrossRef] [Google Scholar] [Publisher Link]
[28] S.D. Sartale, and C.D. Lokhande, "Growth of Copper Sulphide Thin Films by Successive Ionic Layer Adsorption and Reaction (SILAR) Method," *Materials Chemistry and Physics*, vol. 65, no. 1, pp. 63-67, 2000. [CrossRef] [Google Scholar] [Publisher Link]
[29] Samantha Prabath Ratnayake et al., "SILAR Deposition of Metal Oxide Nanostructured Films," *Nano Micro Small*, vol. 17, no. 49, pp. 1-32, 2021. [CrossRef] [Google Scholar] [Publisher Link]
[30] Daichi Tonagi, Manabu Hagiwara, and Shinobu Fujihara, "Fabrication of Highly (1 1 1)-Oriented Cu_2O Films on Glass Substrates by Repeated Chemical Bath Deposition," *Journal of Crystal Growth*, vol. 551, 2020. [CrossRef] [Google Scholar] [Publisher Link]
[31] F.T. Munna et al., "Effect of Zinc Doping on the Optoelectronic Properties of Cadmium Sulphide (CdS) Thin Films Deposited by Chemical Bath Deposition by Utilising an Alternative Sulphur Precursor," *Optik*, vol. 218, 2020. [CrossRef] [Google Scholar] [Publisher Link]
[32] Raid A. Ismail, Abdul-Majeed E. Al-Samarai, and Faris M. Ahmed, "Optoelectronic Properties of n-Ag_2S Nanotubes/p-Si Heterojunction Photodetector Prepared by Chemical Bath Deposition Technique: An Effect of Deposition Time," *Surfaces and Interfaces*, vol. 21, 2020. [CrossRef] [Google Scholar] [Publisher Link]
[33] Jung-Hoon Yu et al., "The Effect of Ammonia Concentration on the Microstructure and Electrochemical Properties of NiO Nanoflakes Array Prepared by Chemical Bath Deposition," *Applied Surface Science*, vol. 532, 2020. [CrossRef] [Google Scholar] [Publisher Link]
[34] Myo Zin Tun et al., "Improving Morphology and Optoelectronic Properties of Ultra-Wide Bandgap Perovskite via Cs Tuning for Clear Solar Cell and UV Detection Applications," *Scientific Reports*, vol. 13, no. 1, pp. 1-12, 2023. [CrossRef] [Google Scholar] [Publisher Link]
[35] Qian Zhao et al., "Improving the Photovoltaic Performance of Perovskite Solar Cells with Acetate," *Scientific Reports*, vol. 6, no. 1, pp. 1-10, 2016. [CrossRef] [Google Scholar] [Publisher Link]
[36] Junaid Younus et al., "Engineering the Optical Properties of Nickel Sulphide Thin Films by Zinc Integration for Photovoltaic Applications," *RSC Advances*, vol. 13, no. 39, pp. 27415-27422, 2023. [CrossRef] [Google Scholar] [Publisher Link]
[37] Jeong-Hyeok Im et al., "Nanowire Perovskite Solar Cell," *Nano Letters*, vol. 15, no. 3, pp. 2120-2126, 2015. [CrossRef] [Google Scholar] [Publisher Link]
[38] Lingling Zheng et al., "Improved Light Absorption and Charge Transport for Perovskite Solar Cells with Rough Interfaces by Sequential Deposition," *Nanoscale*, vol. 6, no. 14, pp. 8171-8176, 2014. [CrossRef] [Google Scholar] [Publisher Link]

[39] Trishala R. Desai et al., "Evaluation of Nanostructured NiS_2 Thin Films from a Single-Source Precursor for Flexible Memristive Devices," *ACS Omega*, vol. 8, no. 51, pp. 48873-48883, 2023. [CrossRef] [Google Scholar] [Publisher Link]

[40] T. Suzuki et al., "Raman Scattering of NiS_2," *Solid State Communications*," vol. 23, no. 11, pp. 847-852, 1977. [CrossRef] [Google Scholar] [Publisher Link]

[41] Chen Dai et al., "Controllable Synthesis of NiS and NiS_2 Nanoplates by Chemical Vapor Deposition," *Nano Research*, vol. 13, no. 9, pp. 2506-2511, 2020. [CrossRef] [Google Scholar] [Publisher Link]

[42] Jeng-Han Wang et al., "Electronic and Vibrational Properties of Nickel Sulfides from First Principles," *The Journal of Chemical Physics*, vol. 127, no. 21, 2007. [CrossRef] [Google Scholar] [Publisher Link]

[43] N. Abhiram et al., "Structural, Vibrational, Morphological, Optical and Electrical Properties of NiS and Fabrication of SnS/NiS Nanocomposite for Photodetector Applications," *Inorganic Chemistry Communications*, vol. 133, 2021. [CrossRef] [Google Scholar] [Publisher Link]